Journal of Engineering Physics and Thermophysics, Vol. 74, No. 1, 2001

POSSIBILITY OF FORMING AN INGOT WITH A CONVEX CRYSTALLIZATION FRONT

Yu. A. Samoilovich, V. I. Timoshpol'skii, and I. A. Trusova

UDC 669.18:548.55

Based on physicomathematical modeling, the feasibility of forming a steel ingot with a convex crystallization front in facilities for directional solidification of ingots (FDSI) has been proved.

It is known that the majority of the liquation defects of the cast structure in steel ingots are concentrated in their axial zone. The damage inflicted by defects on the axial zone is especially evident in continuous casting of steel when the depth of the liquid crater (nonsolidified portion of the ingot) attains 5–10 m [1–5].

In production of steel ingots in remelting furnaces (electroslag remelting furnaces, vacuum arc remelting furnaces), a sharp decrease in the speed of casting (smelting of ingots) and the beneficial effect of refining slag (in electroslag remelting furnaces) or vacuum slag (in vacuum arc remelting furnaces) make it possible to improve radically the technological properties of the produced cast steel [6–8]. However, for large and, especially, superlarge ingots (with a mass of more than 80–120 ton) the problem of the quality of the axial zone of the ingots again becomes rather urgent.

Therefore, the idea of a technological process in which the crystallization front of the melted ingot is plane (there is no crater) or even convex in the direction of smelting has arisen. It is envisioned that this idea be implemented in a facility for directional solidification of ingots, a schematic diagram of which is presented in Fig. 1.

According to the schematic diagram given in the figure, the configuration of the crystallization front of the ingot is governed by the simultaneous effect of two factors: 1) cooling of the ingot surface by the water-cooled elements of the crucible; 2) evolution of induction heat produced by the electric energy of the crucible winding. In the absence of the second factor, a traditional crystallization front in the form of a more or less deep crater (a concave crystallization front) results. But if the evolution of induction heat in the surface layer of the ingot exceeds the cooling effect of the crucible, formation of a plane or even convex crystallization front is feasible. The configuration of the front is governed by the relationship between the heat fluxes, one of which is directed toward the cooled bottom of the ingot and the other depends on the induction heat evolution. In other words, the evolution of induction heat in the surface layer of the ingot heats up the surface or partially melts its solid crust, whereas heat removal along the ingot axis (from top to bottom, from the crystallization front to the ingot bottom) persists and governs the buildup of the solid crust in the axial zone.

In an FDSI, an ingot is formed in a water-cooled crucible integrated with a magnetic-field inductor. Initially, the cavity formed by the ingot mold plate and the crucible walls is filled with a primary batch of the melt. Thereafter, the melt is poured in batches, with the amount of each (or the height of the elementary layers Δh of the melt added) being one of the controlled parameters. From the first minutes of the period of stay of the melt in the crucible, a thin crust of steel ingot forms on its interior surface, which can be melted

Belarusian State Polytechnic Academy, Minsk, Belarus. Translated from Inzhenerno-Fizicheskii Zhurnal, Vol. 74, No. 1, pp. 134–138, January–February, 2001. Original article submitted July 21, 2000.

 1062-0125/01/7401-0192$25.00

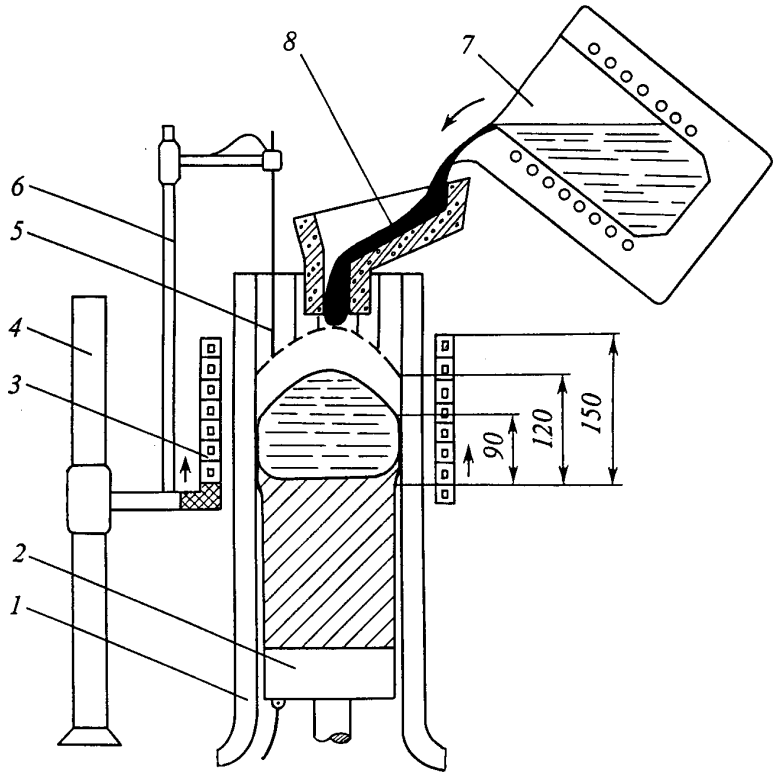

Fig. 1. Schematic diagram of smelting of an ingot in an FDSI facility: 1) cold crucible-crystallizer; 2) ingot mold plate; 3) inductor; 4) mechanism displacing the inductor; 5) tungsten-tantalum electrode; 6) arm; 7) electric furnace; 8) trough.

when the inductor is switched on (due to the Joule heat). As the ingot is built up in the cold crucible, the inductor is displaced so that the Joule heat is evolved in the upper (head) portion of the ingot, and this gives the profile of the crystallization front required by the technological indices for the cast steel. In this scheme of forming an ingot the regime of crystallization is governed by the following factors:

a) the speed of buildup of the ingot $v_{\text{ing}} = \Delta h/\Delta t$;

b) the speed of inductor ascent v_{ind};

c) the electric power of the inductor P;

d) the initial superheating of the melt supplied to the crystallizer;

e) the intensity of the heat removal from the ingot surface to the water-cooled elements of the crucible.

Moreover, the regime of ingot crystallization depends on the dimensions of its cross section and the thermophysical properties of the steel: thermal conductivity λ, heat capacity c, density ρ, specific heat of crystallization L, and the end points of the crystallization range (T_{liqs}, T_{sols}). All these factors were taken into account in posing the problem of the regime of ingot solidification.

Below we present a variant of calculation of the process of formation of a steel ingot with a stable convex surface front of crystallization.

The physicomathematical formulation of the problem [9, 10] includes an equation of nonstationary heat conduction with account for the heat sources in the solidifying melt:

$$\rho c \frac{\partial T}{\partial t} = \operatorname{div}(\lambda \operatorname{grad} T) + Q_{\text{ind}} + Q_{\text{ph}}, \tag{1}$$

where Q_{ind} and Q_{ph} are the volume densities of the heat sources produced by the action of the inductor and the evolution of the heat of phase change. According to [9], the parameter Q_{ph} is considered to be directly proportional to the rate of crystalline growth of the steel:

$$Q_{ph} = \rho L \frac{\partial \psi}{\partial t}, \tag{2}$$

where $\psi = V_s/V_0$ is the relative fraction of the solid phase in the control element of the ingot. Using the substitution $\frac{\partial \psi}{\partial t} = \frac{\partial \psi}{\partial T}\frac{\partial T}{\partial t}$, we reduce Eq. (1) to the form

$$\rho c_{eff}(T) \frac{\partial T}{\partial t} = \text{div}\,(\lambda\ \text{grad}\ T) + Q_{ind}, \tag{3}$$

in which

$$c_{eff}(T) = \begin{cases} c_{liq} & \text{for} \quad T > T_{liqs}; \\ c_{sol} - L\dfrac{d\psi}{dT} & \text{for} \quad T_{sols} < T < T_{liqs}; \\ c_{sol} & \text{for} \quad T < T_{sols}. \end{cases} \tag{4}$$

The derivative $\partial\psi/\partial T$ is called the rate of crystallization; it depends on the form of the phase diagram of the alloy (steel) under study. In the simplest case [9]

$$-\frac{d\psi}{dT} = \frac{1}{T_{liqs} - T_{sols}}.$$

Equation (3) is supplemented with the boundary conditions of the problem:

$$-\left(\lambda \frac{\partial T}{\partial n}\right)_{sur} = \alpha_i (T_{sur} - T_{med}), \tag{5}$$

where n is the direction of the normal to the cooled surface of the ingot, α_i is the local value of the heat-transfer coefficient, which in the general case is different for the ingot mold plate and the side surface of the cold crucible (i = 1 or 2 depending on whether the side or bottom surface of the ingot is studied), and T_{med} is the temperature of the cooled water in the channels of the cold crucible. Equation (3) involves div (divergence) and grad (gradient) symbols. We will make Eq. (3) explicit for the cases of a Cartesian coordinate system (x, y, z) and a cylindrical coordinate system (r, z) assuming axial symmetry of the temperature field:

a) in a Cartesian coordinate system

$$\rho c_{eff}(T) \frac{\partial T}{\partial t} = \frac{\partial}{\partial x}\left(\lambda \frac{\partial T}{\partial x}\right) + \frac{\partial}{\partial y}\left(\lambda \frac{\partial T}{\partial y}\right) + \frac{\partial}{\partial z}\left(\lambda \frac{\partial T}{\partial z}\right) + Q_{ind}, \tag{6}$$

b) in a cylindrical coordinate system

$$\rho c_{eff}(T) \frac{\partial T}{\partial t} = \frac{1}{r}\frac{\partial}{\partial r}\left(\lambda r \frac{\partial T}{\partial r}\right) + \frac{\partial}{\partial z}\left(\lambda \frac{\partial T}{\partial z}\right) + Q_{ind}. \tag{7}$$

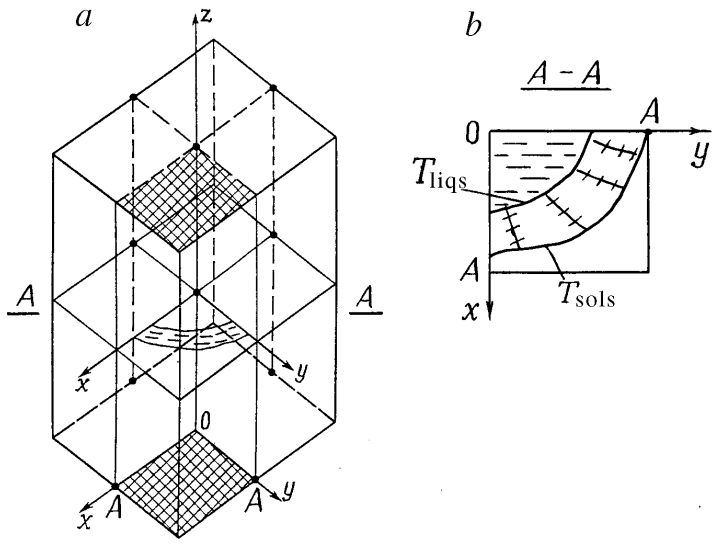

Fig. 2. Scheme of the isolated computational volume (a) in the ingot section (cross-hatched) and the location of the liquidus and solidus isotherms in the ingot cross section (b).

The source of the electric-energy power Q_{ind} is represented in Eqs. (6) and (7) as a function of the coordinate $\bar{x}$ (along the normal to the ingot surface) according to the exponential law

$$Q_{ind} = \frac{2}{\Delta} S_0 \exp\left(-2\frac{\bar{x}}{\Delta}\right), \tag{8}$$

in which $S_0 = kP/L_{ing}H$ is the heat-flux density and Δ is the depth of penetration of the electromagnetic field, which depends on the current frequency f. Thus, $\Delta = 0.0186$ m for $f = 1000$ Hz. The parameter H in Eq. (8) is the height of the active part of the inductor, L_{ing} is the ingot perimeter, k is an empirical constant that characterizes the fraction of the energy produced by the inductor that is absorbed by the ingot (k = 0.25–0.35).

Figure 2 presents the scheme of isolation of a computational volume that is one-fourth of the ingot section with a square cross section (a) and the position of the two-phase zone (b) in the cross section of the ingot: the two-phase zone is a mixture of dendrite crystals and the melt; it is bounded in space by the isotherms of the liquidus ($T = T_{liqs}$) and solidus ($T = T_{sols}$) of the melt under study.

The coordinate origin $x = 0$, $y = 0$ in the scheme of Fig. 2 is placed on the axis of symmetry of the ingot; in this case the distance of x from the ingot surface is calculated from the difference $x = A - x$, with $2A$ being the size of a side of the square cross section of the ingot (similarly $y = A - y$). For one quadrant of the ingot cross section the boundary conditions of the problem become

$$\frac{\partial T}{\partial x} = 0 \quad \text{for} \quad x = 0\,, \quad \frac{\partial T}{\partial y} = 0 \quad \text{for} \quad y = 0\,;$$

$$-\lambda \frac{\partial T}{\partial x} = \alpha\,(T_{sur} - T_{med}) \quad \text{for} \quad x = A\,; \quad -\lambda \frac{\partial T}{\partial y} = \alpha\,(T_{sur} - T_{med}) \quad \text{for} \quad y = A\,. \tag{9}$$

Correspondingly, the following boundary conditions were used in solving the problem in the cylindrical coordinate system:

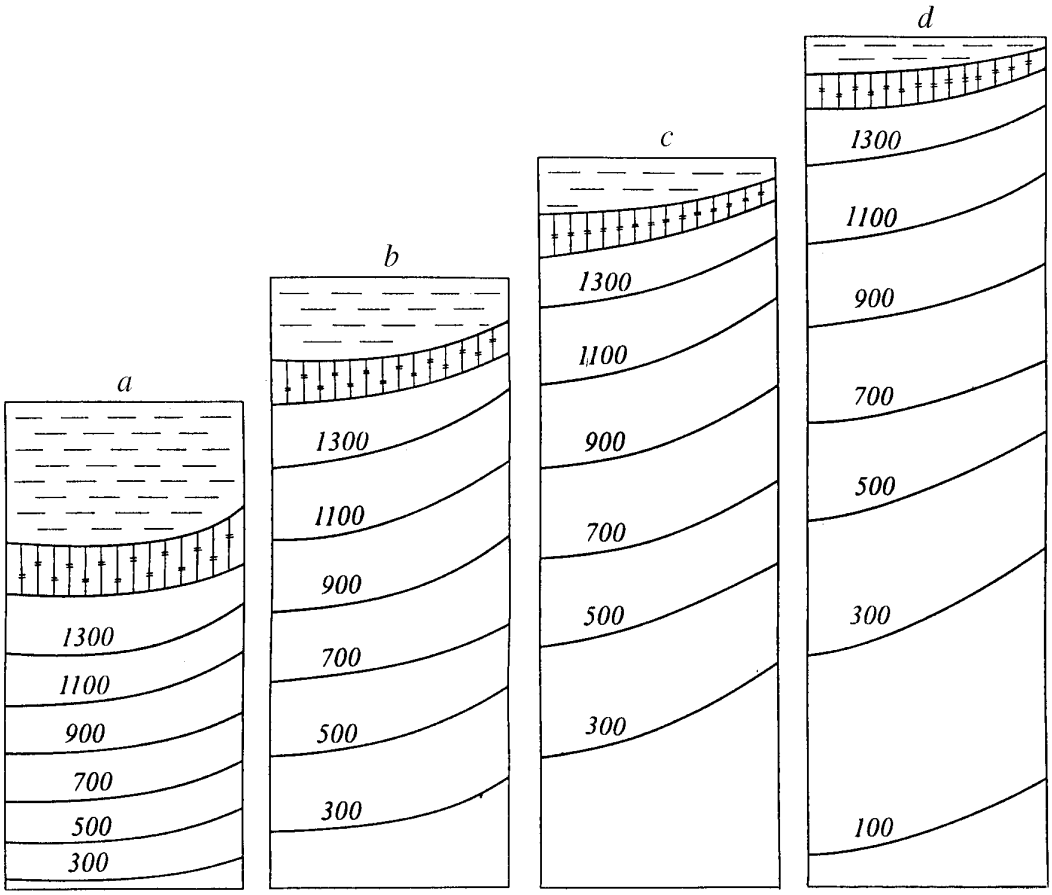

Fig. 3. Location of isotherms in a longitudinal cross section of a square ingot ($2A$ = 0.12 m) with a buildup speed v_{ing} = 5 mm/min and S_0 = $4 \cdot 10^5$ W/m^2 for four instants of time: τ = 330 sec (a), 700 sec (b) 1080 sec (c), and 1440 sec (d).

$$\frac{\partial T}{\partial r} = 0 \quad \text{for} \quad r = 0\,; \quad -\lambda \frac{\partial T}{\partial r} = \alpha\,(T_{sur} - T_{med}) \quad \text{for} \quad r = R\,, \tag{10}$$

where R is the radius of a circular ingot. The boundary conditions (9) or (10) are supplemented with the initial condition of the problem:

$$T = T_m \quad \text{for} \quad t = 0\,, \tag{11}$$

where T_m is the prescribed temperature of the melt entering the cold crucible at the initial instant of time.

In specific calculations, the results of which are given below, the heat-transfer coefficient α was varied within the limits 120–250 W/(m^2·K), and the temperature of the melt was taken equal to $T_m = T_{liqs} + \Delta T_m$, where ΔT_m is the specified initial superheating of the melt (50–80 deg).

The above problem was solved by a grid method (a finite-difference method) based on subdivision of the computational element of the ingot into a set of elements of dimensions Δx, Δy, and Δz (or Δr and Δz) and replacement of continuous time by a sequence of computational intervals (Δt). This was done using an implicit finite-difference scheme [11].

In carrying out the calculations, the dimensions of the cross section of the square ingots were taken to be 0.12 × 0.12 m; the circular ingots had a radius of 0.1 m; the speeds of buildup of the ingots were 2,

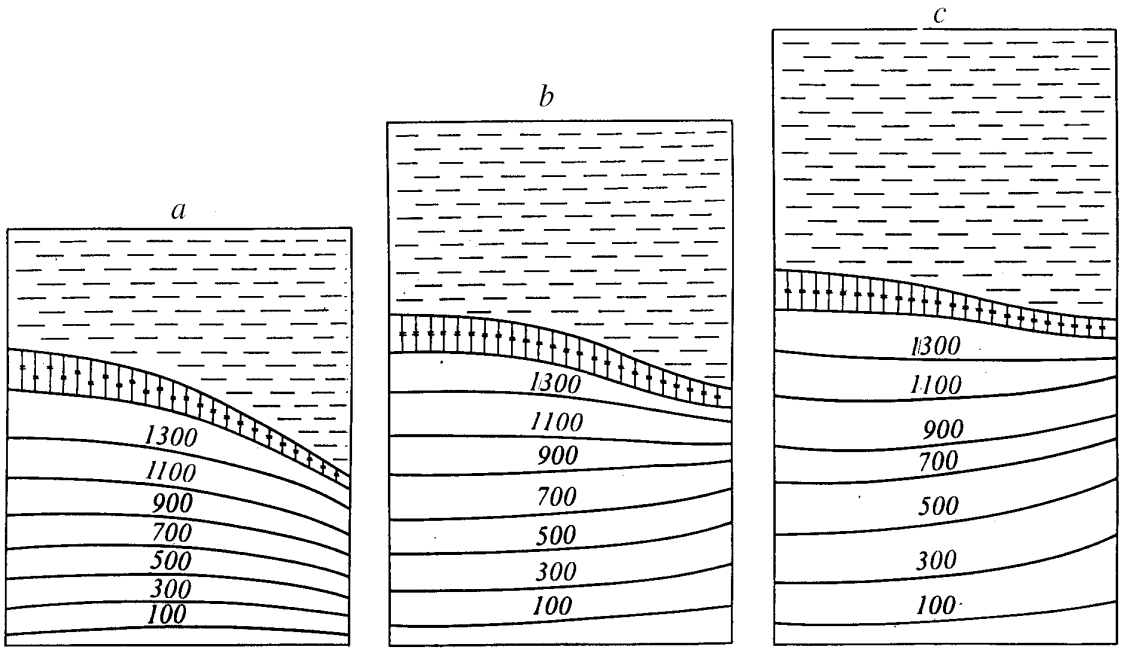

Fig. 4. Location of isotherms in a longitudinal cross section of a circular ingot ($2R$ = 0.12 m) with a buildup speed v_{ing} = 5 mm/min and $S_0 = 8 \cdot 10^5$ W/m^2 for three instants of time: τ = 360 sec (a), 720 (b), and 1080 (c).

5, and 10 mm/min, respectively. The thermophysical properties of the carbon steel were: ρ_{liq} = 7200 kg/m^3, ρ_{sol} = 7600 kg/m^3, $c_{liq} = c_{sol}$ = 700 J/(kg·K), λ_{liq} = 60 W/(m·K), λ_{sol} = 30 W/(m·K), L = 270,000 J/kg, T_{liqs} = 1500°C, and T_{sols} = 1450°C, which corresponds to about 0.5% content of carbon in the steel.

The crucible-crystallizer was filled with the melt in the following way. Initially, the crucible is filled with a steel melt with a temperature T_{in} = 1525°C until an elevation of 0.12 m is reached; then batches of the melt of height Δh = 0.03 m are poured into the crucible at regular intervals Δt that were: Δt = 15 min at v_{ing} = 2 mm/min, Δt = 6 min at v_{ing} = 5 mm/min, and Δt = 3 min at v_{ing} = 10 mm/min.

The surface density of the energy absorbed by the ingot (S_0) was varied within $10–10^6$ W/m^2, with the height of the active part of the inductor being equal to H = 0.1 m.

Results of the mathematical simulation for square and circular steel ingots are presented in Figs. 3 and 4. Figure 3 shows isotherms in a longitudinal cross section of the square ingot, which allow analysis of the dynamics of the temperature field and the shape of the crystallization front for a speed of ingot buildup v_{ing} = 5 mm/min. Similar patterns for the circular ingot are shown in Fig. 4. Consideration of Figs. 3 and 4 allows the conclusion that a convex crystallization front manifests itself to a high degree in circular ingots, whereas square ingots show a greater aptitude for a plane crystallization front.

To carry out multivariant calculations, we varied the intensity of the external cooling of the ingots, the speed of their buildup, and the surface density of the heat evolved due to the electromagnetic energy of the crucible. Several conclusions can be drawn based on the calculational results obtained:

1. Fluctuations of the parameter S_0 (the heat-flux density due to effect of the the inductor) within the range $4 \cdot 10^5–8 \cdot 10^5$ W/m^2 do not change qualitatively the configuration of the crystallization front, characterized by a convex zone for circular ingots and a plane zone for square ones on the diagrams of the longitudinal cross section of the ingots.

2. A similar remark applies to variation, within justifiable limits, of the mean coefficients of heat transfer from the surfaces of the ingots (α) within the range 120–250 W/(m^2·K).

3. The tendency toward obtaining a convex (or plane) crystallization front becomes more evident when the speed of buildup of the ingots is decreased from 5 to 2 mm/min, but this adjustment of the smelting conditions leads to a lower efficiency of the facility and overexpenditure of electric energy.

It is obvious that the choice of an efficient speed for the buildup of ingots and the electric power of the inductor must be verified for specific industrial conditions with account for the evaluated extent to which the steel is free of various chemical and structural inhomogeneities. At the same time, analysis of the calculations carried out shows that an FDSI can produce a practically plane or slightly concave crystallization front in steel ingots of the indicated dimensions (0.12–0.2 m), which is needed to attain a high degree of chemical and structural homogeneity of the cast steel, if the speed of casting (buildup) is maintained at the level of 3–7 mm/min for an inductor power P = 60–80 kW.

NOTATION

T, temperature; T_{liqs}, liquidus temperature; T_{sols}, solidus temperature; T_{med}, temperature of the medium; T_{sur}, surface temperature; T_m, temperature of the melt; ΔT_m, heating of the melt; Q, volume density of the heat source; t, time; v, velocity; Δh, height of a melt batch; V_{sol}, volume of the solid phase in the control element of the ingot; V_0, total volume of the control element of the ingot; ψ, relative fraction of the solid phase; α, heat-transfer coefficient; x, y, z, and r, coordinates; $\bar{x}$, coordinate along the normal to the ingot surface; Δx, Δy, Δz, and Δr, steps in the coordinate; Δt, time step; A, dimension of a side of a square ingot; R, radius of a cylindrical ingot; k, empirical coefficient; P, electric power of the inductor; L_{ing}, perimeter of the ingot; H, height of the active part of the inductor. Subscripts: eff, effective; liq, liquid; sol, solid; sols, solidus; liqs, liquidus; m, melt, med, medium; sur, surface; ind, inductor; ph, phase change; ing, ingot.

REFERENCES

1. A. I. Manokhin, *Production of Homogeneous Steel* [in Russian], Moscow (1978).
2. D. P. Evteev and I. N. Kolybalov, *Continuous Steel Casting* [in Russian], Moscow (1984).
3. A. I. Chizhikov, *Continuous Casting of Steel into Billets of Large Cross Section* [in Russian], Moscow (1970).
4. V. I. Timoshpol'skii, *Heat-Technological Foundations of Metallurgical Processes and Facilities of Higher Technical Level* [in Russian], Minsk (1995).
5. V. Timoshpol'skii (Timoshpolsky), Yu. Feoktistov, I. Trusova, et al., *Operating Experience with VOEST-ALPINE Steelmaking Facility at Byelorussian Metallurgical Plant, in: Proc. 6th Int. Continuous Casting Conf.*, Linz, Austria (1993).
6. B. E. Paton and B. I. Medovar, *Electroslag Technology* [in Russian], Kiev (1976).
7. A. B. Sergeev, F. I. Shved, and N. A. Tulin, *Vacuum Arc Remelting of Structural Steel* [in Russian], Moscow (1974).
8. A. S. Kalugin, *Electron-Beam Melting of Metals* [in Russian], Moscow (1980).
9. Yu. A. Samoilovich, *Forming an Ingot* [in Russian], Moscow (1977).
10. Yu. A. Samoilovich, *Systems Analysis of Ingot Crystallization* [in Russian], Kiev (1983).
11. A. A. Samarskii, *Theory of Difference Schemes* [in Russian], Moscow (1977).